A Synthetic-Eddy-Method to represent the ambient turbulence in numerical simulation of marine current turbine

Clément Carlier, Grégory Pinon, Benoît Gaurier, Grégory Germain, Elie Rivoalen

A Synthetic-Eddy-Method to represent the ambient turbulence in numerical simulation of marine current turbine

Clément Carlier*†, Grégory Pinon*, Benoît Gaurier†, Grégory Germain† and Élie Rivoalen*§
*Laboratoire Ondes et Milieux Complexes (LOMC), UMR 6294, CNRS – Université du Havre,
E-mail: gregory.pinon@univ-lehavre.fr
†IFREMER, Marine Structures Laboratory
E-mails: {clement.carlier, benoit.gaurier, gregory.germain}@ifremer.fr
§Laboratoire d'Optimisation et Fiabilité en Mécanique des Structures (LOFIMS), EA 3828, INSA de Rouen,
E-mail: elie.rivoalen@insa-rouen.fr

***Abstract*—The development of marine current turbines arrays has been an active research topic for some years. However, many studies are still necessary in order to fully understand the behaviour of such arrays. One of these studies is the impact of the ambient turbulence on the behaviour of marine current turbines. Indeed recent studies have shown that ambient turbulence intensity highly modifies the behaviour of horizontal axis marine current turbines. Consequently numerical simulations have to represent the ambient turbulence or at least its effects on the performance and wake of the turbines. This paper presents the latest numerical developments carried out at LOMC in collaboration with IFREMER in order to take into account the effects of ambient turbulence.**

***Index Terms*—Turbulence, Marine current turbine, Numerical computations, Synthetic-Eddy-Method, Wake, Performance.**

I. Introduction

The development of marine current turbines arrays has been an active research topic for some years [1]–[3]. However, many studies are still necessary in order to fully understand the behaviour of such array. One of these studies is the impact of the ambient turbulence on the behaviour of marine current turbines. Indeed recent studies have shown that ambient turbulence intensity I_∞ (see eq. (1)) highly modifies the behaviour of horizontal axis marine current turbines [4]–[7].

$$I_\infty = 100\sqrt{\frac{\frac{1}{3}[\sigma^2(u_\infty)+\sigma^2(v_\infty)+\sigma^2(w_\infty)]}{\bar{u}_\infty^2+\bar{v}_\infty^2+\bar{w}_\infty^2}} \quad (1)$$

One of the most noticeable influence can be observed in the wake, downstream of the turbine. Indeed as shown in Fig. 1, the higher the turbulence intensity I_∞ is, the faster the wake effects decrease. Moreover the interactions between turbines are also highly modified by the effect of the ambient turbulence as shown by Mycek *et al.* [8] in their study of the performances and wake of two interacting turbines.

It reveals crucial to accurately characterise the influence that different levels of ambient turbulence I_∞ have on tidal turbine. Indeed, several *in situ* studies have shown that ambient turbulence may vary between 3.2% [9] and 10.3% [10], or even more (see [8]) in some other potential tidal sites. The relative spread in ambient turbulence levels inhibits the definition of general guidelines on tidal arrays with respect to turbulence. Therefore, the influence of each level of ambient turbulence needs to be characterised, either experimentally or numerically.

Consequently numerical simulations have to represent the ambient turbulence, or at least its effects on the performance and wake of the turbines. The point here is not to describe a turbulence model (like in RANS, LES or DES models) but to generate accurate turbulent inflow conditions that represent a given ambient turbulence level. Some numerical works were carried out in that aim. For example, Chatelain *et al.* [11] used the Mann's algorithm [12] to synthesise a turbulent inflow in the case of wind turbines simulations. As for marine current turbines simulations, Togneri *et al.* [13], [14] already investigated a similar Synthetic-Eddy-Method in order to generate synthetic turbulent inflow conditions for their BEMT software.

This paper presents the latest numerical developments carried out in order to take into account the effects of ambient turbulence. Therefore a new module was integrated to the three-dimensional software developed at LOMC [15]. This software already possesses an LES turbulent model, its turbulent eddy viscosity being based on the work of Mansour et al. [16]. The new module, based on the Synthetic-Eddy-Method developed by Jarrin *et al.* [17], [18], was initially dedicated to the production of inflow conditions for Eulerian Large-Eddy Simulations. The present work intends to apply this SEM model to the Lagrangian Vortex Method framework.

The first part of this paper is devoted to the presentation of the numerical method used to compute the flow around three bladed horizontal axis marine current turbines. Then in a second part, the Synthetic-Eddy-Method is presented as well as its integration in the present software. The last part of this paper focuses on preliminary results obtained using this method to represent the ambient turbulence I_∞. Eventually, conclusions are drawn on the presented work and an outlook on future numerical work is given.

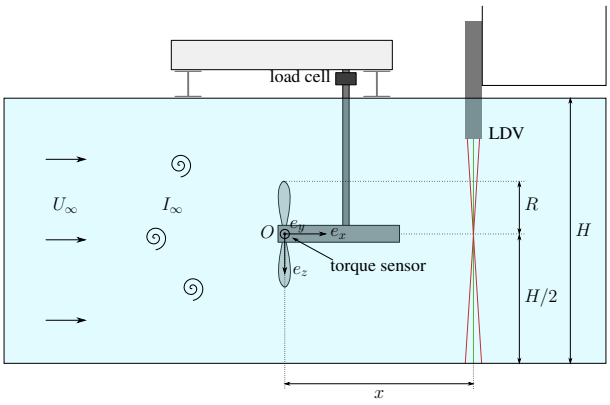

(a) Sketch of the experimental set-up

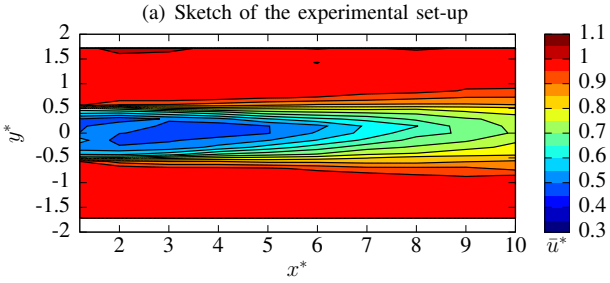

(b) Wake, $I_\infty = 3\%$

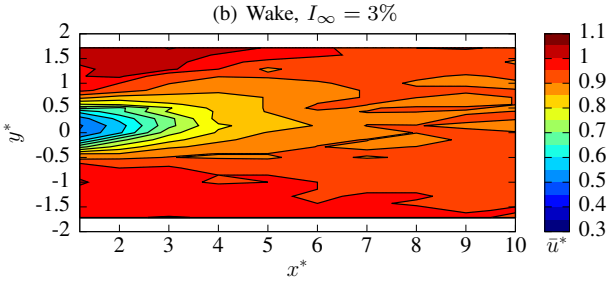

(c) Wake, $I_\infty = 15\%$

Fig. 1. Sketch of the experimental set-up reproduced from [8]. Wake behind a turbine with TSR $= 3.67$, $U_\infty = 0.8\text{m.s}^{-1}$ for different ambient turbulence intensity I_∞ [6]. The turbine centre is located at the coordinate (0;0), x^* (*resp.* y^*) stands for x/D (*resp.* y/D), D stands for the turbine diameter and $\bar{u}^*$ represents the dimensionless velocity deficit calculated as $\bar{u}/U_\infty$.

II. Numerical method

The software developed to simulate marine current turbines is based on the Vortex method [19]–[21]. This method is an unsteady Lagrangian method, where the flow is discretised using vorticity carrying particles and the turbines are represented using a panel method [22]. In this numerical method, the Navier-Stokes equations for an unsteady and incompressible flow are used in their velocity/vorticity $(\vec{u}, \vec{\omega})$ formulation:

$$\nabla \cdot \vec{u} = 0, \tag{2}$$

$$\frac{D\vec{\omega}}{Dt} = \left(\vec{\omega} \cdot \nabla\right) \vec{u} + \nu \Delta \vec{\omega}, \tag{3}$$

where $\vec{u}$ is the velocity field, $\vec{\omega} = \nabla \wedge \vec{u}$ is the vorticity field and ν is the kinematic viscosity. Equation (3) basically represents the momentum equation in the velocity-vorticty formulation. $\left(\vec{\omega} \cdot \nabla\right) \vec{u}$ stands for the stretching term and $\nu \Delta \vec{\omega}$ for diffusion. Thanks to viscous splitting (see Chap. 5 of Cottet & Koumoutsakos [21]), diffusion is handled via a Particle Strength Exchange model initially developed by Degond & Mas-Gallic [23] and Choquin & Huberson [24]. Additionally, an LES model with a turbulent eddy viscosity based on the work of Mansour *et al.* [16] completes the numerical model for diffusion. One can refer to [15] for more detailed information.

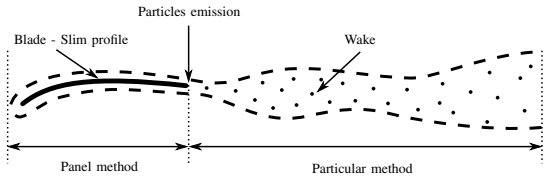

Fig. 2. Decomposition of the Vortex method.

The Helmholtz decomposition of the velocity field (eq. (4)) is used in order to decompose the velocity vector:

$$\vec{u} = \nabla \wedge \vec{\psi} + \nabla\phi + \vec{u}^{\infty} = \vec{u}^{\psi} + \vec{u}^{\phi} + \vec{u}^{\infty}, \tag{4}$$

Thus the velocity field is divided into three parts:

- a potential component $\vec{u}^{\phi}$ representing the influence of the turbines blades on the flow (see Fig. 2). This component $\vec{u}^{\phi}$ of the velocity field is obtained using a panel method [22] to solve

  $$\Delta\phi = 0. \tag{5}$$

  This previous equation (5) is obtained by introducing equation (4) in the continuity equation (eq. (2)). One can refer to [25] in order to have the latest numerical developments on that part of the software.
- a rotational component $\vec{u}^{\psi}$ representing the wake of the turbines (see Fig. 2). The component $\vec{u}^{\psi}$ is the solution of the equation

  $$\Delta\vec{\psi} = -\vec{\omega}, \tag{6}$$

  obtained by introducing the Helmholtz decomposition (eq. (4)) in the vorticity definition $\vec{\omega} = \nabla \wedge \vec{u}$.
- a velocity vector $\vec{u}^{\infty}$ representing the upstream tidal current.

In order to make the link between the rotational and the potential parts of the velocity, particles are emitted at the blade's trailing edge thanks to a Kutta-Joukowski condition [15], [26], [27]. The emitted particles are then advected in the flow as shown in Fig. 2. The emission scheme was recently modified to take into account more precisely the influence of the turbine blades feet. Thanks to those modifications an improvement of the near wake representation (≤ 4 diameters) was achieved.

The particles emitted at the trailing edge of the blades represent the downstream wake of the turbines (see Fig. 2). The rotational part $\vec{u}^{\psi}$ of the velocity field is calculated as the sum of the influence of these vorticity carrying particles. The expression of the component $\vec{u}^{\psi}$ is obtained in every point M of the fluid domain by solving the equation (6) thanks to the Biot and Savart law [27], [28]:

$$\overrightarrow{\boldsymbol{u}}^{\psi}(M) = \frac{1}{4\pi}\sum_{i=1}^{N}\frac{\overrightarrow{\boldsymbol{MX_i}}}{|\overrightarrow{\boldsymbol{MX_i}}|^3}\wedge\overrightarrow{\boldsymbol{\Omega}}_i, \tag{7}$$

with $\overrightarrow{\boldsymbol{OX_i}}$ the position of the particle i, $\overrightarrow{\boldsymbol{MX_i}}$ the vector going from any point M of the domain to the particle i, $\overrightarrow{\boldsymbol{\Omega}}_i$ the vorticity carried by this particle i and N the total number of particles in the flow. The evaluation of this component $\overrightarrow{\boldsymbol{u}}^{\psi}$ for each particles represent the major part of the computational cost. For that reason, a *Treecode* algorithm inspired from Lindsay and Krasny [29] is used to reduce the computational time. For more details on the computations, including regularisation of equation (7), remeshing or time-stepping, etc., one can refer to [15], [27].

III. Synthetic-Eddy-Method

The Synthetic-Eddy-Method proposed by Jarrin *et al.* [17], [18] is investigated in this study in order to represent the ambient turbulence effects thanks to the above mentioned 3D software. For instance, this method was already adapted by Togneri *et al.* [14] to their BEMT code for tidal turbines. The Synthetic-Eddy-Method was initially developed to generate an input flow with a given turbulence intensity I_∞ and a given anisotropic ratio (σ_u:σ_v:σ_w) by adding a perturbation term, which is added to the mean velocity of the flow $\overrightarrow{\boldsymbol{u}}^{\infty}$.

A. General overview of the method

Similarly to a Reynolds decomposition of the velocity, a fluctuating term $\overrightarrow{\boldsymbol{u}}^{\sigma}$ is added to the upstream mean velocity $\overrightarrow{\overline{\boldsymbol{u}}^{\infty}}$ and the upstream tidal current velocity $\overrightarrow{\boldsymbol{u}}^{\infty}$ then becomes:

$$\overrightarrow{\boldsymbol{u}}^{\infty}(\overrightarrow{\boldsymbol{x}}) = \overrightarrow{\overline{\boldsymbol{u}}^{\infty}} + \overrightarrow{\boldsymbol{u}}^{\sigma}(\overrightarrow{\boldsymbol{x}}) \tag{8}$$

On the contrary to the already presented method [17], [18], this perturbation term is not only added at the inlet of the fluid domain but everywhere in the studied space. But this aspect will be treated later in sub-sec. III-B.

This perturbation term $\overrightarrow{\boldsymbol{u}}^{\sigma}$ is calculated as the influence of N generated "turbulent structures", also called "eddies", randomly placed in the studied space. Then the perturbation term $\overrightarrow{\boldsymbol{u}}^{\sigma}$ induced by those N turbulent structures is simply defined as the sum of the influences of each structure k:

$$\overrightarrow{\boldsymbol{u}}^{\sigma}(\overrightarrow{\boldsymbol{x}}) = \sum_{k=1}^{N}\overrightarrow{\boldsymbol{u}}^{\sigma,k}(\overrightarrow{\boldsymbol{x}}), \tag{9}$$

with $\overrightarrow{\boldsymbol{x}}$ being any point of the flow and $\overrightarrow{\boldsymbol{u}}^{\sigma,k}$ the velocity induced by a single turbulent structure k. This velocity can be expressed as:

$$\overrightarrow{\boldsymbol{u}}^{\sigma,k}(\overrightarrow{\boldsymbol{x}}) = \sqrt{\frac{V_\sigma}{N}}\overrightarrow{\boldsymbol{c}}^{k}F_{\overrightarrow{\boldsymbol{\lambda}}}(\overrightarrow{\boldsymbol{x}} - \overrightarrow{\boldsymbol{x}}^{k}) \quad \forall k \in [\![1, N]\!], \tag{10}$$

where V_σ is the volume of the three-dimensional space containing all the N "turbulent structures". At this point, the turbulent structure k and more particularly its intensity $\overrightarrow{\boldsymbol{c}}^{k}$ needs to be defined together with the function $F_{\overrightarrow{\boldsymbol{\lambda}}}$.

Each turbulent structure k is defined by its position $\overrightarrow{\boldsymbol{x}}^{k}$ in the flow and its intensity $\overrightarrow{\boldsymbol{c}}^{k}$. The intensity $\overrightarrow{\boldsymbol{c}}^{k}$ is defined as:

$$c_i^k = \sum_{j=1}^{3} a_{i,j}\epsilon_{i,j}^k \quad \forall i \in \{1,2,3\}, \quad \forall k \in [\![1, N]\!]. \tag{11}$$

The different $\epsilon_{i,j}^k$ terms that intervene in equation (11) are independent random values that follow a normal or Gaussian distribution centred around 0 with a variance of 1. This $\epsilon_{i,j}^k$ term is supposed to represent the random aspect of turbulence. The elements $a_{i,j}$ represents any element of a matrix A, which is basically the Cholesky decomposition of the Reynolds Stress Tensor $\overline{\overline{\boldsymbol{R}}}$ (see eq. (12)).

$$\overline{\overline{\boldsymbol{R}}} = \begin{pmatrix} R_{1,1} & R_{1,2} & R_{1,3} \\ R_{2,1} & R_{2,2} & R_{2,3} \\ R_{3,1} & R_{3,2} & R_{3,3} \end{pmatrix} = \overline{\overline{\boldsymbol{A}}}\overline{\overline{\boldsymbol{A}}}^{T} \quad \text{with} \quad \overline{\overline{\boldsymbol{A}}} = \left(a_{i,j}\right) \tag{12}$$

Thanks to these equations (11) and (12), the link between the intensities $\overrightarrow{\boldsymbol{c}}^{k}$ of the turbulent structures and the Reynolds Stress Tensor $\overline{\overline{\boldsymbol{R}}}$ ensures the generation of a velocity field that statistically replicates any given turbulence intensity I_∞ and any given anisotropic ratio (σ_u:σ_v:σ_w) [17], [30]. Indeed the three components of the anisotropic ratio (σ_u:σ_v:σ_w) are just the square root of the diagonal components over the component R_{11} of the Reynolds Stress Tensor $\overline{\overline{\boldsymbol{R}}}$. Moreover the turbulence intensity I_∞ expression can be rewritten in function of the trace of the Reynolds Stress Tensor $\overline{\overline{\boldsymbol{R}}}$ as shown in equation (13):

$$\begin{aligned} I_\infty &= 100\sqrt{\frac{\frac{1}{3}[\sigma^2(u_\infty)+\sigma^2(v_\infty)+\sigma^2(w_\infty)]}{\bar{u}_\infty^2+\bar{v}_\infty^2+\bar{w}_\infty^2}} \\ &= \frac{100}{|\overrightarrow{\boldsymbol{u}}^{\infty}|}\sqrt{\frac{R_{1,1}+R_{2,2}+R_{3,3}}{3}} \\ &= \frac{100}{|\overrightarrow{\boldsymbol{u}}^{\infty}|}\sqrt{\frac{\mathbf{tr}\left(\overline{\overline{\boldsymbol{R}}}\right)}{3}} \end{aligned} \tag{13}$$

This last equation (13) ensures that the generated turbulence will have the desired turbulence intensity I_∞ and the desired anisotropic ratio (σ_u:σ_v:σ_w).

The second part of equation (10) is $F_{\overrightarrow{\boldsymbol{\lambda}}}$ also called the shape function and it can be express as:

$$F_{\overrightarrow{\boldsymbol{\lambda}}}(\overrightarrow{\boldsymbol{y}}) = \prod_{i=1}^{3} f_{\lambda_i}(y_i). \tag{14}$$

$\overrightarrow{\boldsymbol{\lambda}}$ defines the size of the zone of influence of each turbulent structure k. This size could naively (and maybe erroneously) be interpreted as a turbulent length scale (Taylor or Kolmogorov length scales) but this will need further investigation. As it is defined by a vector $\overrightarrow{\boldsymbol{\lambda}}$, and presented in equation (14), the zone of influence can ideally have different sizes regarding each coordinate (λ_i). Ideally, each turbulent structure could have its own size $\overrightarrow{\boldsymbol{\lambda}}$ but this needs to be further investigated. However, in the present implementation, all turbulent structures share the same size vector $\overrightarrow{\boldsymbol{\lambda}}$ and unless mentioned are isotropic. The sub-functions f_λ that intervene in the evaluation of the shape function $F_{\overrightarrow{\boldsymbol{\lambda}}}$ have to meet some

conditions to ensure that the ambient turbulence has the chosen characteristics:

$$\underset{y}{\operatorname{argmax}}(f_\lambda(y)) = 0, \tag{15a}$$

$$f_\lambda(y) = f_\lambda(-y), \tag{15b}$$

$$\int_{-\lambda}^{\lambda} (f_\lambda^2(y)dy = 1. \tag{15c}$$

In the preliminary results presented in section IV, the basic shape function $F_{\overrightarrow{\boldsymbol{\lambda}}}$ (eq. (14)) indicated in Jarrin *et al.* [17], [18] is used. Indeed its sub-function f_λ basically is a tent function, represented by a triangular function centered at zero with a base of 2λ.

$$f_\lambda(y) = \begin{cases} \sqrt{\frac{3}{2\lambda^3}}(\lambda - |y|) & \text{if} \quad |y| < \lambda \\ 0 & \text{otherwise.} \end{cases} \tag{16}$$

Figure 3 depicts tent functions for different values of λ.

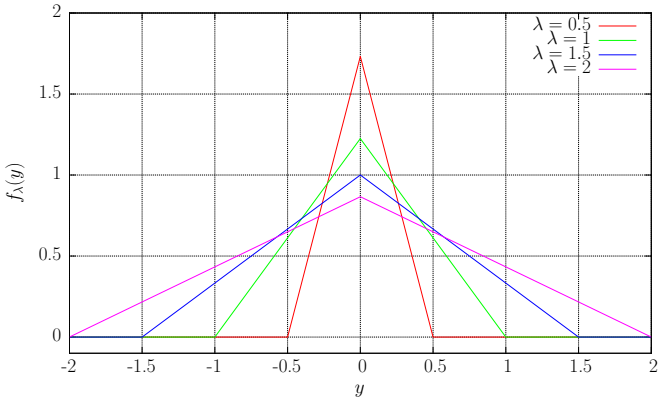

Fig. 3. The tent function for different sizes λ of turbulent structure.

It is anticipated that this basic tent function (eq. 16) will not meet all the requirement of smoothness, especially if ones want to computed the velocity gradient, etc. However, in order to start with, this basic function issued from the bibliography will be used.

B. Integration of the Synthetic-Eddy-Method into the Vortex method

The numerical method presented in section II is by definition an unsteady Lagrangian method on an unbounded domain. Indeed, the fluid domain is supposed to be infinite but the zone where particles are present, grows with the particles emission and their advection in the flow. In fact, there is no domain boundaries as in Eulerian formulation. Unfortunately the Synthetic-Eddy-Method need the definition of a precise volume V_σ (see eq. (10)) containing all the turbulent structures, which is not required for classical Vortex method. Thus in order to combine the Synthetic-Eddy-Method with the Vortex method, a studied space E_S needed to defined. The desired velocity fluctuations induced by the Synthetic-Eddy-Method will be applied inside this E_S domain.

Once the studied space E_S is defined, a turbulent space E_σ of volume V_σ can be created. This turbulent space E_σ contains all the turbulent structures used in the Synthetic-Eddy-Method. If one wants to have a statistically correct velocity fluctuations everywhere inside the studied space E_S, some conditions on the turbulent space E_σ are needed, especially at the limit. Therefore, the turbulent space E_σ needs to be a little larger than the studied space E_S:

$$\min(x_i \in E_\sigma) \leq \min(x_i \in E_S) - \lambda_i \quad \forall i \in \{1,2,3\}, \tag{17a}$$

$$\max(x_i \in E_\sigma) \geq \max(x_i \in E_S) + \lambda_i \quad \forall i \in \{1,2,3\} \tag{17b}$$

with $\overrightarrow{\boldsymbol{x}}$ a position vector and $\overrightarrow{\boldsymbol{\lambda}} = \lambda_i$, $(i = 1,3)$ the size vector of the turbulent structures. Those conditions simply ensure that all the study space is influenced by the turbulent structures.

Now that the turbulent space E_σ is defined, the generation of the turbulent structures can be performed. E_σ is initialised with the N turbulent structures k and their intensities $\overrightarrow{\boldsymbol{c}}^k$ are calculated using equation (11) with $\epsilon_{i,j}^k$ taking the value 1 with a probability of $1/2$ and the value -1 with an equal probability. Then each turbulent structure is randomly placed in the turbulent space E_σ.

During the simulation, the turbulent structures will be advected by the flow. Here, different strategies can be applied: either the structures can be advected by $\overrightarrow{\boldsymbol{u}}^\infty$, which is somehow too simplistic, or the structures can be advected by $\overrightarrow{\boldsymbol{u}}$ as defined in equation (4). Additionally, these structures could also be used in order to compute the stretching term of the Navier-Stokes equation (first term of the right end side of equation (3)) but not presented here. In this preliminary study, the first option was chosen that is: the structures are advected by $\overrightarrow{\boldsymbol{u}}^\infty$ without influencing the stretching term. These structures work somehow as an under-layer, which means that they will influence the velocity distribution on the turbines (and hence the particles emission process) and also the particles in the wake. But they will not be influenced reciprocally.

Regarding the second option (the structures are advected by the actual fluid velocity $\overrightarrow{\boldsymbol{u}}$), several questions arise. In fact, the validity of the method relies on the randomness of the turbulent structures locations; will this property still be valid when advected by $\overrightarrow{\boldsymbol{u}}$? Thus, with the second approach, the Synthetic-Eddy-Method may not replicate the prescribed Reynolds stress tensor. Some more work needs to be perform on that prior to choose this second option.

Finally during the advection of the turbulent structures, each structure leaving the turbulent space E_σ will be suppressed and replaced by a newly generated one at the inlet of the turbulent space E_σ.

IV. Numerical results

The numerical results presented in this section are issued from preliminary computations and will only be used as proof of concept. At first, the ambient turbulence module will be run without any turbine to ensure that model correctly reproduces

the different input parameters. Then, a computation will be presented with the presence of a single turbine for a moderate turbulence intensity I_∞ level.

A. Results on the ambient turbulence model without turbine

The ambient turbulence module was firstly studied without turbine to ensure that the model correctly reproduces the different input parameters such as the turbulence intensity I_∞ and the anisotropic ratio (σ_u:σ_v:σ_w). This verification is quite straight forward as I_∞, σ_u, σ_v and σ_w can be deduced from the Reynolds Stress Tensor $\overline{\overline{\boldsymbol{R}}}$ (see eq. (13)).

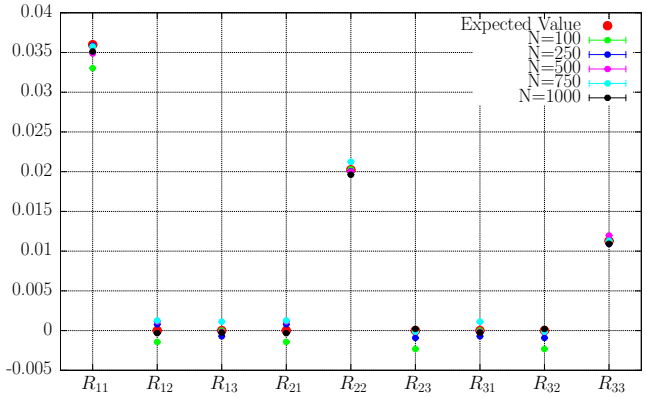

Fig. 4. Comparison between values of the Reynolds Stress Tensor $\overline{\overline{\boldsymbol{R}}}$ (see eq. (12)) prescribed to the model and the ones obtained with the Synthetic-Eddy-Method at $I_\infty = 15\%$ for different number N of turbulent structures of size $\lambda_i = (1.0, 1.0, 1.0)$.

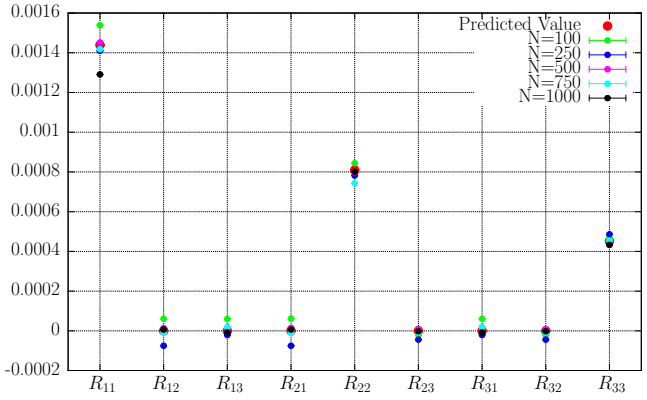

Fig. 5. Comparison between values of the Reynolds Stress Tensor $\overline{\overline{\boldsymbol{R}}}$ (see eq. (12)) prescribed to the model and the ones obtained with the Synthetic-Eddy-Method at $I_\infty = 3\%$ for different number N of turbulent structures of size $\lambda_i = (1.0, 1.0, 1.0)$.

In that aim, 3D turbulent velocity fields were generated on a fluid domain E_S of dimensionless size $6 \times 6 \times 6$. In order to validate the model, the generated flow-field characteristics are analyzed. Figures 4 to 7 give examples of comparison between the Reynolds Stress Tensor $\overline{\overline{\boldsymbol{R}}}$ prescribed to the model and the one recalculated from the generated flow. These four examples are for diagonal Reynolds Stress Tensors $\overline{\overline{\boldsymbol{R}}}$, which correspond to an ambient turbulent I_∞ of 15% and 3%

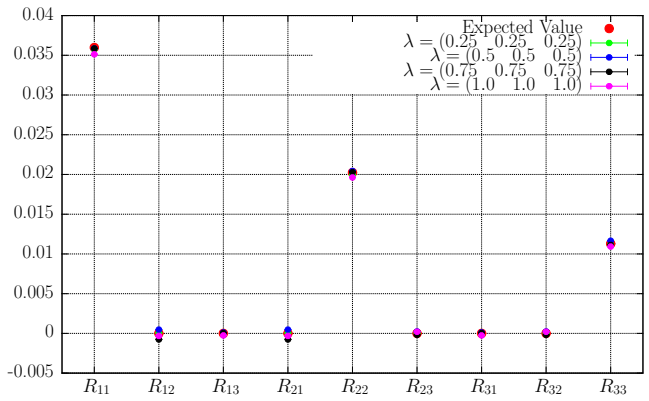

Fig. 6. Comparison between values of the Reynolds Stress Tensor $\overline{\overline{\boldsymbol{R}}}$ (see eq. (12)) prescribed to the model and the ones obtained with the Synthetic-Eddy-Method at $I_\infty = 15\%$ with $N = 1000$ structures and for different turbulent structures of sizes λ.

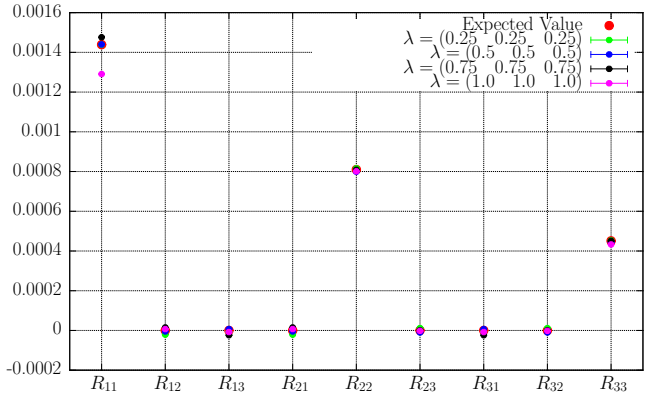

Fig. 7. Comparison between values of the Reynolds Stress Tensor $\overline{\overline{\boldsymbol{R}}}$ (see eq. (12)) prescribed to the model and the ones obtained with the Synthetic-Eddy-Method at $I_\infty = 3\%$ with $N = 1000$ structures and for different turbulent structures of sizes λ.

respectively. The anisotropic ratio was arbitrarily set to the one observed in Milne *et al.* [10]. On these Figures 4 to 7, the values recomputed from the generated flow show an excellent agreement with the prescribed ones and thus regardless of the number of used turbulent structures or their size. This good agreement between the prescribed and recomputed values of the Reynolds Stress Tensor $\overline{\overline{\boldsymbol{R}}}$ proves the model capacity to generate velocity fluctuations replicating a given turbulence intensity I_∞ and anisotropic ratio (σ_u:σ_v:σ_w).

Figure 8 displays the results obtained with the Synthetic-Eddy-Method for different values of ambient turbulence. It shows example of "turbulent" flow-field generated with the model for the same anisotropic ratio (σ_u:σ_v:σ_w)=(1.0,0.75,0.56) and different turbulence intensities I_∞. One can observe that the generated flow seems to be very realistic, although all the proper turbulence characteristics are not taken into account. Additionally, even though the turbulent structures sizes were equally set to $\lambda_i = (1.0, 1.0, 1.0)$, this length cannot be clearly observed only looking at the velocity field.

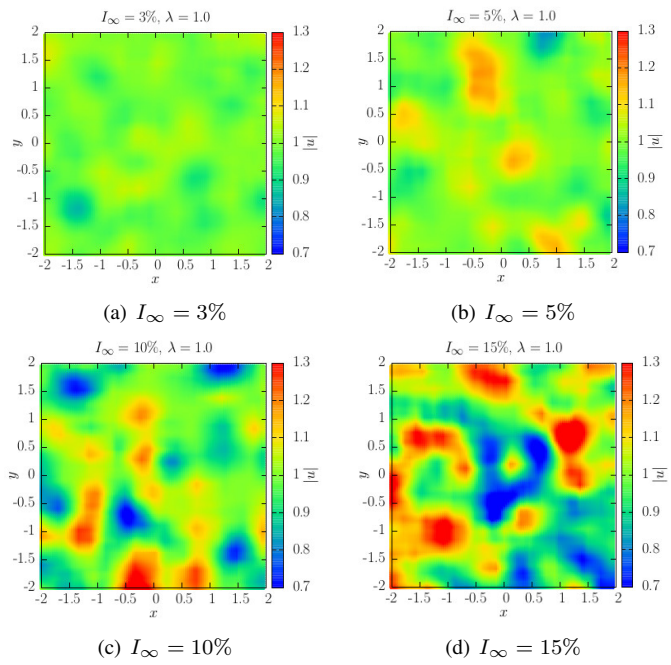

(a) $I_\infty = 3\%$ (b) $I_\infty = 5\%$

(c) $I_\infty = 10\%$ (d) $I_\infty = 15\%$

Fig. 8. Examples of velocity field provided by the ambient turbulence model for $N = 1000$ structures of size $\lambda_i = (1.0, 1.0, 1.0)$ and different values of I_∞.

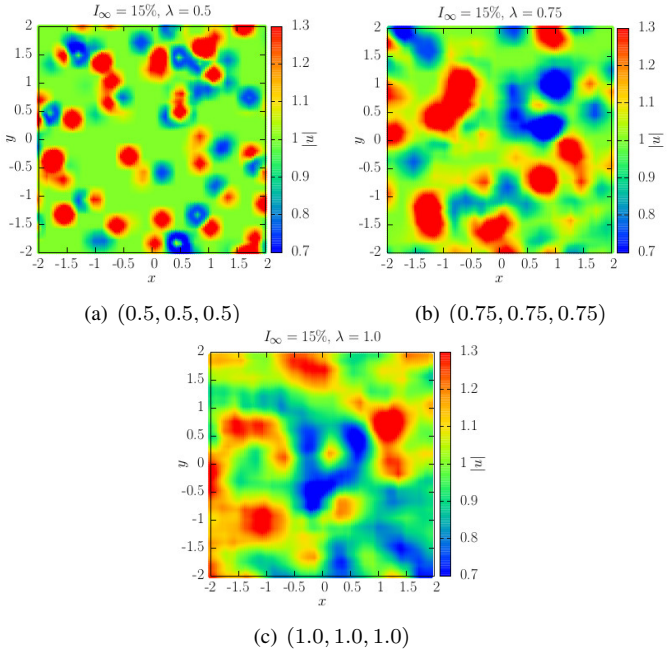

(a) $(0.5, 0.5, 0.5)$ (b) $(0.75, 0.75, 0.75)$

(c) $(1.0, 1.0, 1.0)$

Fig. 9. Example of velocity field provided by the ambient turbulence model for $I_\infty = 15\%$, $N = 1000$ structures and different structure sizes.

The turbulent structures size $\overrightarrow{\lambda}$ is revealed to be an important parameter for this Synthetic-Eddy-Method and its influence needs to be further investigated. Figure 9 displays flow-field generated by the model for three sizes of structure. The differences between those three flow-field are quite striking. Indeed, when the turbulent structures are small, each independent structure can be clearly identified, and the larger they get, the more difficult it is to locate them as they are superposing themselves.

A complete study of the different intervening parameters is under progress. The main parameters to be assessed are the turbulent structure size $\overrightarrow{\lambda}$, the number N of required turbulent structures for a given volume V_σ of E_σ, etc. Fluctuation velocity spectra are also envisaged in order to better characterise the Synthetic-Eddy-Method such as in [31].

B. Results using the ambient turbulence model on a single turbine

Further to the previous study of turbulent flow without any turbine, a few computations were run with a turbine. Those tests were run for a turbulent intensity I_∞ of 3%, the lowest turbulent intensity value for which experimental results are accessible in the IFREMER wave and current flume tank. The obtained results are very encouraging and a qualitative analysis can already be performed.

Figures 10 and 11 depict the numerically computed wakes for $I_\infty = 0\%$ as in ref. [15] and for $I_\infty = 3\%$ similarly to the experiments performed by Mycek *et al.* [8]. The experimental wake is also presented as a matter of comparison. The Tip Speed Ratio TSR-value is set to 2.5. The turbulent parameters were arbitrary set to $\overrightarrow{\lambda} = (0.2, 0.2, 0.2)$, $N = 2000$ in a fluid domain E_S that goes from -1 to 12.5 in the x direction and from -2.5 to 2.5 in the y and z directions.

The velocity maps presented on Figure 10 seem to indicate that the velocity deficit is underestimated in the numerical wakes for both without and with ambient turbulence set to $I_\infty = 3\%$. This underestimation could partially be attributed to the fact that, since now, only rather coarse computations were performed. With finer discretisations, better velocity deficit are expected as already obtained in [15]. However, taking a closer look on the velocity profiles presented in the Figure 11, one can see that numerical computation already give a fair estimation of the velocity profiles in the wake of the turbine.

Moreover the numerical velocity profiles presented in Figure 11 at 2, 3 and 5 diameters downstream of the turbine show that even a low ambient turbulence intensity of 3% already have an effect on the wake. Indeed the ambient turbulence model seems to have a smoothing effect on the near wake, one of the best example being the smoothing of the velocity deficit peak owing the hub of the turbine at $x = 2D$ downstream (and $x = 3D$ to a smaller extend). The disappearance of this velocity deficit peak is a qualitative improvement of the turbine near wake as this velocity peak does not clearly appear on the experimental velocity profiles. However, with the addition of ambient turbulence, the computation further reduces the velocity deficit (especially at $x = 2D$ and $3D$) which is not in accordance with the experiments. As already mentioned, these are only preliminary results which need to be further validated with more computations (finer discretisations, a mesh independence analysis, etc.). Hopefully, in a near future, more intense turbulent conditions are scheduled (higher turbulence

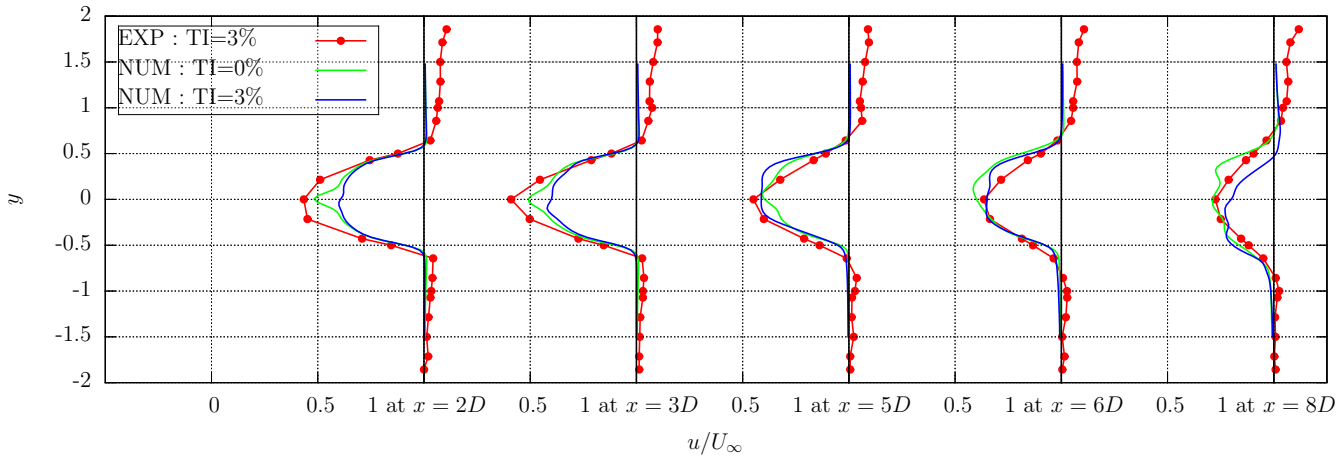

Fig. 11. Numerical and experimental comparison of axial velocity profiles downstream of a three bladed horizontal axis marine current turbines at TSR $= 2.5$ and $I_\infty = 3\%$.

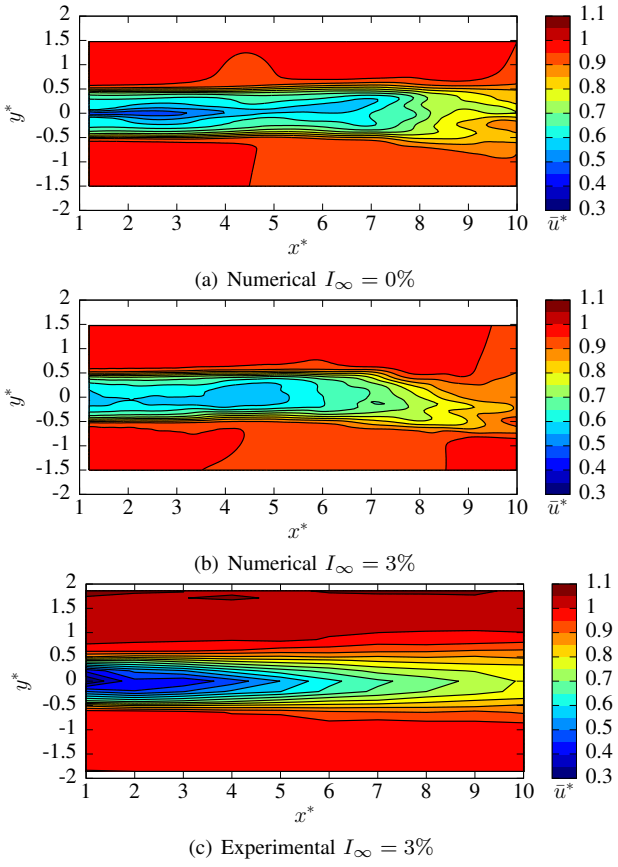

(a) Numerical $I_\infty = 0\%$

(b) Numerical $I_\infty = 3\%$

(c) Experimental $I_\infty = 3\%$

Fig. 10. Velocity maps in the wake downstream a three bladed turbine at TSR $= 2.5$. The center of the turbine is located at the coordinate (0;0).

intensities and possibly anisotropic cases) in order to cover the whole ambient turbulence intensity range ($3\% \leq I_\infty \leq 15\%$).

V. Conclusions and Further works

The important role played by the ambient turbulence intensity on marine current turbines' behaviour was addressed thanks to a numerical investigation. The works carried out at LOMC in partnership with IFREMER in order to better represent the influence of the ambient turbulence in numerical computations was introduced. Indeed, a new module based on this Synthetic-Eddy-Method initially proposed by Jarrin *et al.* [17], [18] was implemented in the numerical code in order to represent the ambient turbulence around marine current turbines. The general characteristics of the Synthetic-Eddy-Method were presented together with its integration in the framework of a 3D unsteady Lagrangian Vortex method.

The capability of the ambient turbulence model to reproduce a perturbed flow that verifies any turbulence intensity I_∞ and any anisotropic ratio (σ_u:σ_v:σ_w) was validated. Moreover the compatibility of the presented ambient turbulence model with the use of a turbine on the software was proven and first results in terms of turbine wake were presented.

As a matter of short-term perspective, a better qualification of the Synthetic-Eddy-Method is needed in order to better understand the input parameters of the model. For instance, the role of the shape function need to be identified and improvement are already planned. In fact, the present function is really simplistic with a major inconvenience. Indeed, the first derivative of a tent function is not continuous and not defined for the value $-\lambda$, 0 and λ. And as already mentioned, the velocity gradients are necessary for the evaluation of the stretching term of the Navier-Stokes equation. One possible shape function candidate correcting this inconvenient could be a Gaussian function with a compact support.

Another development on the ambient turbulence model could be the modification of the Synthetic-Eddy-Method in order to generate a divergence-free flow. In fact, divergence-free flow is a compulsory hypothesis inherent to the Vortex

method in order to apply the Biot & Savart law. Unfortunately, the present implementation is for sure not divergence-free. For low to moderate turbulence intensities, this should introduce a tremendous error in the flow but increasing the turbulence intensity might become an issue. Such kind of development were already initiated by Poletto *et al.* [32] but need a lot of work in order to be introduced in the framework of Vortex method.

However, in the meantime, the next step in this study is to perform a complete numerical investigation of a marine current turbine and confront the numerical results obtained with experimental data [6] for $I_\infty = 3\%$ and $I_\infty = 15\%$. The final goal of this study being the computation of an entire farm of marine current turbines for any turbulent intensity is hard challenge. This hard challenge is however treated step by step, as the other paper proposed by Carlier *et al.* [25] wish to treat the numerical treatment of turbines in a farm.

ACKNOWLEDGMENT

The authors would like to thank Haute-Normandie Regional Council and Institut Carnot IFREMER Edrome for their financial supports for C. Carlier Ph.D. Grant and "GRR Energie" programs. The authors also would like to thank the CRIHAN (Centre des Ressources Informatiques de Haute-Normandie) for their available numerical computation resources.

REFERENCES

[1] R. Malki, I. Masters, A. Williams, and T. Croft, "The influence on tidal stream turbine spacing on performance," in *9th European Wave and Tidal Energy Conference (EWTEC)*, September 2011, Southampton, UK.

[2] L. Myers and A. Bahaj, "An experimental investigation simulating flow effects in first generation marine current energy converter arrays," *Renewable Energy*, vol. 37, no. 1, pp. 28–36, 2012. [Online]. Available: http://www.sciencedirect.com/science/article/pii/S0960148111001716

[3] P. Mycek, B. Gaurier, G. Germain, G. Pinon, and E. Rivoalen, "Numerical and experimental study of the interaction between two marine current turbines," *International Journal of Marine Energy*, vol. 1, no. 0, pp. 70 – 83, 2013. [Online]. Available: http://www.sciencedirect.com/science/article/pii/S2214166913000088

[4] T. Blackmore, W. M. Batten, G. U. Műller, and A. S. Bahaj, "Influence of turbulence on the drag of solid discs and turbine simulators in a water current," *Experiments in Fluids*, vol. 55, no. 1, 2013. [Online]. Available: http://dx.doi.org/10.1007/s00348-013-1637-9

[5] L. Myers, K. Shah, and P. Galloway, "Design, commissioning and performance of a device to vary the turbulence in a recirculating flume," in *10th European Wave and Tidal Energy Conference (EWTEC)*, September 2013, Aalborg, Denmark.

[6] P. Mycek, B. Gaurier, G. Germain, G. Pinon, and E. Rivoalen, "Experimental study of the turbulence intensity effects on marine current turbines behaviour. part I: One single turbine," *Renewable Energy*, vol. 66, no. 0, pp. 729 – 746, 2014. [Online]. Available: http://www.sciencedirect.com/science/article/pii/S096014811400007X

[7] O. D. Medina, F. Schmitt, R. Calif, G. Germain, and B. Gaurier, "Turbulence et intermitence dans les énergies mmarine : mesures à haute fréquence en laboratoire de la relation entre puissance produite par une hydrolienne et turbulence," in *14èmes Journées de l'Hydrodynamique*, Novembre 2014, val de Reuil, France.

[8] P. Mycek, B. Gaurier, G. Germain, G. Pinon, and E. Rivoalen, "Experimental study of the turbulence intensity effects on marine current turbines behaviour. part II: Two interacting turbines," *Renewable Energy*, vol. 68, no. 0, pp. 876 – 892, 2014. [Online]. Available: http://www.sciencedirect.com/science/article/pii/S0960148114000196

[9] J. MacEnri, M. Reed, and T. Thiringer, "Influence of tidal parameters on seagen flicker performance," *Philosophical Transactions of the Royal Society A: Mathematical, Physical and Engineering Sciences*, vol. 371, no. 1985, p. pp, February 2013. [Online]. Available: http://rsta.royalsocietypublishing.org/content/371/1985/20120247.abstract

[10] I. A. Milne, R. N. Sharma, R. G. J. Flay, and S. Bickerton, "Characteristics of the turbulence in the flow at a tidal stream power site," *Philosophical Transactions of the Royal Society A: Mathematical, Physical and Engineering Sciences*, vol. 371, no. 1985, p. pp, February 2013. [Online]. Available: http://rsta.royalsocietypublishing.org/content/371/1985/20120196.abstract

[11] P. Chatelain, S. Backaert, G. Winckelmans, and S. Kern, "Large eddy simulation of wind turbine wakes," *Flow Turbulence and Combustion*, vol. 91, pp. 587–605, 2013.

[12] J. Mann, "The spatial structure of neutral atmosphere surface-layer turbulence," *Journal of Fluid Mechanics*, vol. 273, pp. 141–168, 1994.

[13] M. Togneri and I. Masters, "Parametrising turbulent marine flows for a blade element momentum model of tidal stream turbines," in *9th European Wave and Tidal Energy Conference (EWTEC)*, September 2011, Southampton, UK.

[14] ——, "Synthetic turbulence generation for turbine modelling with BEMT," in *3rd Oxford Tidal Energy Workshop*, Oxford, UK, 7-8 April 2014.

[15] G. Pinon, P. Mycek, G. Germain, and E. Rivoalen, "Numerical simulation of the wake of marine current turbines with a particle method," *Renewable Energy*, vol. 46, no. 0, pp. 111 – 126, 2012. [Online]. Available: http://www.sciencedirect.com/science/article/pii/S0960148112002418

[16] N. Mansour, J. Ferziger, and W. Reynolds, "Large-eddy simulation of a turbulent mixing layer," Report TF-11, Thermosciences Div., Dept. of Mech. Eng., Stanford University, Tech. Rep., 1978.

[17] N. Jarrin, S. Benhamadouche, D. Laurence, and R. Prosser, "A synthetic-eddy-method for generating inflow conditions for large-eddy simulations," *International Journal of Heat and Fluid Flow*, vol. 27, pp. 585–593, 2006.

[18] N. Jarrin, "Synthetic inflow boundary conditions for the numerical simulation of turbulence," Ph.D. dissertation, University of Manchester, 2008.

[19] C. Rehbach, "Calcul numérique d'écoulements tridimensionnels instationnaires avec nappes tourbillonaires," *La Recherche Aérospatiale*, vol. 5, pp. 289–298, 1977.

[20] R. Lewis, *Vortex element methods for fluid dynamic analysis of engineering systems*. Cambridge University Press, 1991.

[21] G. Cottet and P. Koumoutsakos, *Vortex methods: theory and practice*. Cambridge University Press, 2000.

[22] J. Bousquet, *Méthode des singularités*. Cépaduès - Editions, 1990.

[23] P. Degond and S. Mas-Gallic, "The weighted particle method for convection-diffusion equations. Part I: The case of an isotropic viscosity," *Math. Comp.*, vol. 53, no. 188, pp. 485–507, 1989. [Online]. Available: http://dx.doi.org/10.2307/2008716

[24] J. Choquin and S. Huberson, "Particles simulation of viscous flow," *Computers & Fluids*, vol. 17, no. 2, pp. 397 – 410, 1989. [Online]. Available: http://www.sciencedirect.com/science/article/pii/0045793089900492

[25] C. Carlier, G. Pinon, B. Gaurier, G. Germain, and Élie Rivoalen, "Numerical and experimental study of elementary interactions in marine current turbines array," in *11th European Wave and Tidal Energy Conference (EWTEC)*, September 2015, Nante, France.

[26] F. Hauville and Y. Roux, "Réglage dynamique d'une voile par une méthode d'intéraction fluide/structure," in *9èmes Journées de l'Hydrodynamique*, 2003.

[27] P. Mycek, "étude numérique et expérimentale du comportement d'hydroliennes," Ph.D. dissertation, Université du Havre, 2013.

[28] G. S. Winckelmans and A. Leonard, "Contributions to vortex particle methods for the computation of three-dimensional incompressible unsteady flows," *Journal of Computational Physics*, vol. 109, no. 2, pp. 247–273, 1993. [Online]. Available: http://www.sciencedirect.com/science/article/B6WHY-45P11X4-9/2/18db4eee303171d83ce200e0170c4543

[29] K. Lindsay and R. Krasny, "A particle method and adaptive treecode for vortex sheet motion in three-dimensional flow," *J. Comput. Phys.*, vol. 172, pp. 879–907, 2001.

[30] T. S. Lund, X. Wu, and K. D. Squires, "Generation of turbulent inflow

data for spatially-developing boundary layer simulations," *Journal of Computational Physics*, vol. 140, pp. 233–258, 1998.

[31] O. D. Medina, F. Schmitt, R. Calif, G. Germain, and B. Gaurier, "Correlation between synchronised power and flow measurements, a way to characterize turblence effecs on marine current turbine." in *11th European Wave and Tidal Energy Conference (EWTEC)*, September 2015, Nante, France.

[32] R. Poletto, T. Craft, and A. Revell, "A new divergence free synthetic eddy method for the reproduction of inlet flow conditions for les," *Flow, Turb. and Combustion*, vol. 91, pp. 519–539, 2013.